ELSEVIER

12 March 2001

PHYSICS LETTERS A

Physics Letters A 281 (2001) 34–38

www.elsevier.nl/locate/pla

Multistep cascading and fourth-harmonic generation

Andrey A. Sukhorukov [a], Tristram J. Alexander [a], Yuri S. Kivshar [a,*], Solomon M. Saltiel [b]

[a] *Australian Photonics Cooperative Research Centre, Research School of Physical Sciences and Engineering Optical Sciences Centre, Australian National University, Canberra ACT 0200, Australia*

[b] *Quantum Electronics Department, Faculty of Physics, University of Sofia, Sofia 1164, Bulgaria*

Received 18 September 2000; accepted 26 January 2001
Communicated by A.R. Bishop

Abstract

A concept of multistep cascading is applied to the problem of fourth-harmonic generation (FHG) in a single quadratic crystal, and a new model of parametric wave mixing is analyzed in detail. Important applications to the optical frequency division and efficient FHG as well as the realization of the double-phase-matching multistep cascading processes in engineered QPM structures with phase-reversal sequences are also suggested. © 2001 Elsevier Science B.V. All rights reserved.

OCIS: 190.4410; 190.5530; 190.2620; 190.4160

Cascading effects in optical materials with quadratic (second-order or $\chi^{(2)}$) nonlinear response provide an efficient way to lower the critical power of all-optical switching devices [1]. The concept of *multistep cascading* [2] brings new ideas into this field, leading to the possibility of an enhanced nonlinearity-induced phase shift and generation of multicolor parametric spatial solitons. In particular, multistep cascading can be achieved by two nearly phase-matched second-order nonlinear processes, second-harmonic generation (SHG) and sum-frequency mixing (SFM), involving the third-harmonic wave [3,4].

In this Letter, we extend the concept of multistep cascading to the processes involving the fourth-harmonic generation (FHG) in a single noncentrosymmetric crystal, and analyze a new model of multistep cascading and its stationary solutions for *normal modes* — plane waves and spatial solitons. Our study provides the first analysis of the problem of FHG via a pure cascade process, observed experimentally more than 25 years ago [5] and later studied in a special limit only [6]. Additionally, we demonstrate that engineered QPM structures with phase-reversal sequences can provide an effective mean to verify experimentally many of the multistep cascading effects.

We consider the FHG via two second-order parametric processes: $\omega + \omega = 2\omega$ and $2\omega + 2\omega = 4\omega$, where ω is the frequency of the fundamental wave. In the approximation of slowly varying envelopes with the assumption of zero absorption of all interacting waves, we obtain

$$\frac{\partial A}{\partial z} = \frac{i}{2k_1}\frac{\partial^2 A}{\partial x^2} + i\gamma_1 A^* S e^{-i\Delta k_1 z},$$

$$\frac{\partial S}{\partial z} = \frac{i}{2k_2}\frac{\partial^2 S}{\partial x^2} + i\gamma_1 A^2 e^{i\Delta k_1 z} + i\gamma_2 S^* T e^{-i\Delta k_2 z},$$

* Corresponding author.
E-mail address: ysk124@rsphysse.anu.edu.au (Yu.S. Kivshar).

PII: S0375-9601(01)00106-2

$$\frac{\partial T}{\partial z} = \frac{i}{2k_4}\frac{\partial^2 T}{\partial x^2} + i\gamma_2 S^2 e^{i\Delta k_2 z},$$

where A, S, and T are the envelopes of the fundamental-frequency (FF), second- (SH) and fourth-harmonic (FH) waves, respectively, $\gamma_{1,2}$ are proportional to the elements of the second-order susceptibility tensor, and $\Delta k_1 = 2k_1 - k_2$ and $\Delta k_2 = 2k_2 - k_4$ are the corresponding wave-vector mismatch parameters. We introduce the normalized envelopes (u, v, w) according to the following relations: $A(x,z) = (8L\gamma_2)^{-1} \times u(x/a, z/L)\exp(-i\Delta k_1 z/2)$, $S(x,z) = (4L\gamma_2)^{-1} \times v(x/a, z/L)$, and $T(x,z) = (2L\gamma_2)^{-1} w(x/a, z/L) \times \exp(i\Delta k_2 z)$, where L is a characteristic distance, and $a = \sqrt{L/(2k_1)}$. In order to describe a family of nonlinear modes characterized by the *propagation constant* λ, we look for solutions in the form $u(x,z) \to \lambda U(x\sqrt{|\lambda|}, z|\lambda|)e^{i\lambda z/4}$, $v(x,z) \to \lambda V(x\sqrt{|\lambda|}, z|\lambda|) \times e^{i\lambda z/2}$, and $w(x,z) \to \lambda W(x\sqrt{|\lambda|}, z|\lambda|)e^{i\lambda z}$, and obtain the normalized equations:

$$\begin{aligned}
&is\frac{\partial U}{\partial z} + s\frac{\partial^2 U}{\partial x^2} - \alpha_1 U + \chi U^* V = 0,\\
&2is\frac{\partial V}{\partial z} + s\frac{\partial^2 V}{\partial x^2} - V + V^* W + \frac{\chi}{2}U^2 = 0,\\
&4is\frac{\partial W}{\partial z} + s\frac{\partial^2 W}{\partial x^2} - \alpha W + \frac{1}{2}V^2 = 0. \qquad (1)
\end{aligned}$$

Here $s = \mathrm{sign}(\lambda) = \pm 1$, $\chi = \gamma_1/(4\gamma_2)$ is a relative strength of two parametric processes, and the normalized mismatches are defined as $\alpha = 4 + \beta/\lambda$ and $\alpha_1 = 1/4 + \beta_1/\lambda$, where $\beta = 4\Delta k_2 L$ and $\beta_1 = -\Delta k_1 L/2$.

First, we analyze the plane-wave solutions of Eqs. (1) which do not depend on x. In this case, the total intensity I is conserved, and we present it in terms of the unscaled variables as $I = I_u + I_v + I_w$, where $I_u = |u|^2/4$, $I_v = |v|^2$, and $I_w = 4|w|^2$. Solutions $\{U_0, V_0, W_0\}$, which do not depend on z, are *the so-called normal modes*. The simplest one-component FH mode $\{0, 0, W_0\}$ exists at $\alpha = 0$. It has a fixed phase velocity $\lambda = -\beta/4$ and an arbitrary amplitude, and becomes unstable for $I_w > \beta^2/4$ due to a *parametric decay instability*.

Two-mode solution $\{0, \sqrt{2\alpha}, 1\}$ describes a parametric coupling between SH and FH waves, and it exists for $\alpha \geqslant 0$, bifurcating at $\alpha = 0$ from the FH mode. Coupling of this two-mode plane wave to a FF wave can lead to its decay instability, provided $|\alpha_1| < \alpha_1^{(\mathrm{cr})} = \chi\sqrt{2\alpha}$. To understand the physical meaning of this inequality, we note that the family of solutions characterized by the propagation constant λ corresponds to a straight line in the (α, α_1)-parameter space, see Figs. 1(a) and (b). Moreover, all such lines include the point of the exact phase matching $(4, 1/4)$ as the asymptotic limit for $|\lambda| \to +\infty$. This point belongs to the instability region if the relative strength of the FF–SH interaction exceeds a *critical value*, i.e., for $\chi > \chi^{(\mathrm{cr})} = 1/(8\sqrt{2}) \simeq 0.088$. However, for $\chi < \chi^{(\mathrm{cr})}$ this *decay instability is suppressed* due to a strong coupling with the FH field.

Finally, a three-mode solution, $V_0 = \alpha_1/\chi$, $W_0 = V_0^2/(2\alpha)$, $U_0 = \sqrt{2V_0(1 - W_0)/\chi}$, exists for (i) $\alpha > 0$ and $0 < \alpha_1 < \alpha_1^{(\mathrm{cr})}$, (ii) $\alpha > 0$ and $\alpha_1 < -\alpha_1^{(\mathrm{cr})}$, and (iii) $\alpha < 0$ and $\alpha_1 > 0$. In the limit $|\lambda| \to +\infty$, such three-mode plane waves exist only for $\chi > \chi^{(\mathrm{cr})}$. In region (i), stability properties of the three-wave modes are determined by a simple criterion, $\partial I/\partial|\lambda| > 0$. For the parameter regions (ii) and (iii), oscillatory instabilities are possible as well. Existence and stability of all types of stationary plane-wave solutions of model (1) are summarized in Figs. 1(a)–(d).

In general, system (1) is nonintegrable and its dynamics is irregular. However, we find that in some cases a quasi-periodic energy exchange between the harmonics is possible. Fig. 2(a) shows one such case, when the intensities of unstable two-wave and stable three-wave stationary modes are close to each other, and an unstable two-wave mode periodically generates a FF component. Less regular dynamics is observed for other cases, such as for the generation of both SH and FH waves from an input FF wave (Fig. 2(b)). This example also illustrates the possibility of effective energy transfer to higher harmonics close to the double-phase-matching point.

Eqs. (1) may have a different physical meaning provided the normalized amplitude v stands for the mode of the fundamental frequency ω. Then, Eqs. (1) describe the optical frequency division by two (the field u) via parametric amplification and down-conversion (see, e.g., [7]), provided both FF (v) and SH (w) fields are launched simultaneously at the input. Such a frequency division parametric process is in fact shown in Fig. 2(a), where this time the generated u wave corresponds to the frequency $\omega/2$, and is shown as dotted.

We now look for spatially localized solutions of Eqs. (1), *quadratic solitons*. First, we note that two-

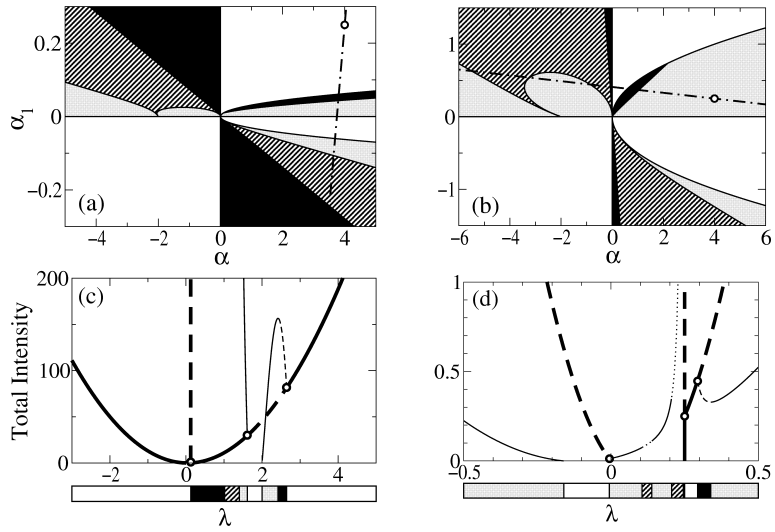

Fig. 1. (a), (b) Existence and stability of three-mode plane waves for (a) $\chi = \chi^{(\mathrm{cr})}/4$ and (b) $\chi = 4\chi^{(\mathrm{cr})}$. Light shading — stable, black — unstable, dark shading — oscillatory unstable, and blank — no solutions. Open circles mark exact phase matching, dash-dotted lines correspond to the lower plots. (c), (d) Intensity versus λ for (c) $\beta = \beta_1 = -0.5$ and (d) $\beta = -1$, $\beta_1 = 0.04$. Thick dashed/solid vertical line — one-wave (FH) modes, thick curves — two-wave (SH + FH) modes, thin curves — three-wave modes. Solid — stable, dashed — unstable, and dotted — oscillatory unstable modes. Open circles mark the bifurcation points. The legend beneath shows the stability of three-wave modes by using the same shadings as in the upper plots.

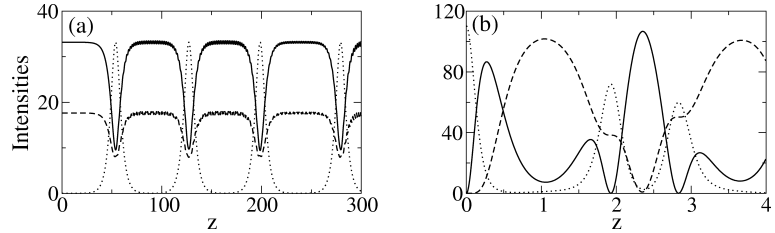

Fig. 2. Dynamics of plane waves: (a) Instability of a two-wave mode (corresponding to $\lambda = 2.1$ in Fig. 1(c)). (b) Generation of higher harmonics from a FF input (parameters are $\chi = 0.625 \simeq 7\chi^{(\mathrm{cr})}$, $\beta = -1$, and $\beta_1 = 0.04$). FF, SH, and FH components are shown by dotted, solid, and dashed curves, respectively.

wave solitons consisting of the SH and FH components can be approximated as [2,8]

$$V_0(x) = V_m \operatorname{sech}^p(x/p),$$
$$W_0(x) = W_m \operatorname{sech}^2(x/p),$$
$$V_m^2 = \frac{\alpha W_m^2}{(W_m - 1)}, \quad \alpha = \frac{4(W_m - 1)^3}{(2 - W_m}, \quad p = \frac{1}{(W_m - 1)}, \tag{2}$$

where all parameters are functions of α only. Bright solitons either do not exist or are unstable being in resonance with linear waves [4] outside the parameter region $\alpha > 0$ and $\alpha_1 > 0$ at $s = +1$. We find that in this region, similar to plane-wave modes, three-wave solitons exist for $0 < \alpha_1 < \alpha_1^{(\mathrm{cr})}$, where the critical (cut-off) value $\alpha_1^{(\mathrm{cr})}$ corresponds to a bifurcation from the two-wave solution (2). In order to find $\alpha_1^{(\mathrm{cr})}$, we should solve the first equation of system (1) with the SH profile from Eqs. (2) (see also [2]). However, such a linear eigenvalue problem has no exact analytical solution for arbitrary p, and thus we introduce an approximation $V_0(x) \simeq \widetilde{V}_0(x) = V_m \operatorname{sech}^2(x/q)$, requir-

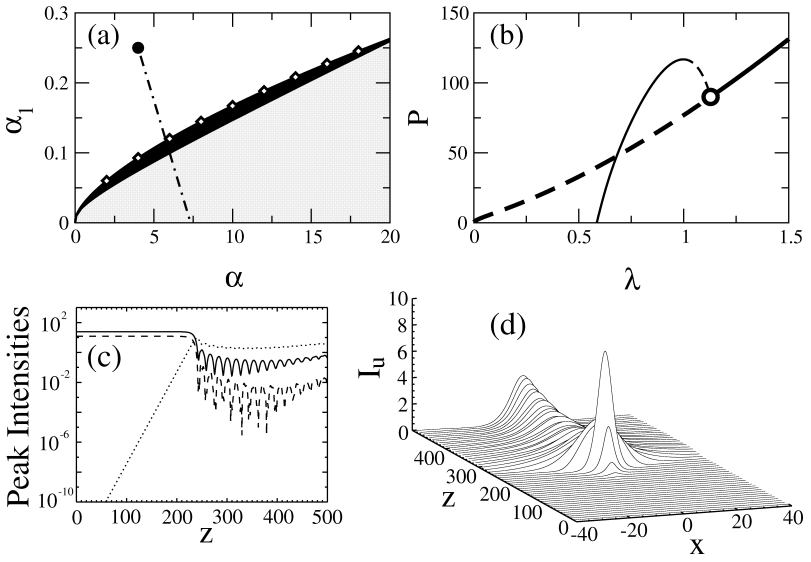

Fig. 3. (a) Regions of existence and stability of three-mode parametric solitons (shading is the same as in Fig. 1(a)). Open diamonds — an analytical approximation, dark circle — exact phase-matching point. The dash-dotted line corresponds to the solutions at $\beta = 2$ and $\beta_1 = -0.15$, for which the power versus λ dependences are shown in (b): thick — two-wave (SH + FH), and thin — three-wave solitons; solid and dashed lines mark stable and unstable solutions, respectively. Open circle is the bifurcation point. (c), (d) Development of a decay instability of a two-wave soliton corresponding to $\lambda = 1$ in (b), and generation of a three-component soliton: (c) FF, SH, and FH peak intensities versus distance shown by dotted, solid, and dashed curves, respectively; (d) evolution of the FF component. For all the plots $\chi = \chi^{(\mathrm{cr})}/2$.

ing that the functions coincide at the amplitude level $V_m/2$, and then define the scaling parameter as $q = p\cosh^{-1}(2^{1/p})/\cosh^{-1}(2^{1/2})$. Such an approximation adequately describes an effective soliton-induced waveguide, and thus should provide overall good accuracy (except for some limiting cases). After solving the eigenvalue problem with the potential $\chi\widetilde{V}_0(x)$, we obtain an approximate expression for the *bifurcation points*:

$$\alpha_1^{(\mathrm{cr})} \simeq \frac{(\sqrt{1+4V_m\chi q^2}-1-2n)^2}{4q^2},$$

where n is the order of the mode guided by the two-component parametric soliton waveguide [2]. For a single-hump mode ($n = 0$) the behavior of this cut-off is very similar to that of the plane waves. Indeed, in the cascading limit ($\alpha \gg 1$), we have $V_m \simeq 2\sqrt{\alpha}$ and $\alpha_1^{(\mathrm{cr})} \simeq 2\chi\sqrt{\alpha}$, which differs by $\sqrt{2}$ from the corresponding result for plane waves. The critical value of χ for one-hump solitons can also be found from the approximate solution, $\chi^{(\mathrm{cr})} \simeq 0.132$. We performed numerical simulations and found that the accuracy of our approximation is of the order of (and usually better than) 1% in a wide range of parameters ($\chi > 10^{-2}$ and $\alpha > 10^{-2}$), see Fig. 3(a), open diamonds. Additionally, similar to other models of multistep cascading [2,4], Eqs. (1) possess various types of *exact analytical solutions*, which will be presented elsewhere.

Quite remarkably, for both positive α and α_1 the stability properties of solitons (see Figs. 3(a) and (b)) and plane waves (see Figs. 1(a) and (c)) look similar. Specifically, stability of two- and three-component solitons is defined by the Vakhitov–Kolokolov criterion $\partial P/\partial\lambda > 0$, where $P = \int_{-\infty}^{+\infty} I\,dx$ is the soliton power, except for the region $\alpha_1 < \alpha_1^{(\mathrm{cr})}$ where two-component solutions exhibit parametric decay instability. An example of such an instability is presented in Figs. 3(c) and (d), where an unstable two-wave soliton generates a stable three-wave state. Such instability-induced dynamics is very different from that of plane waves where, instead, quasi-periodic energy exchange

is observed (see Fig. 2(a)). In the case of localized beams, diffraction leads to an effective power loss and convergence to a new (stable) state.

In order to observe experimentally the multistep cascading and multi-frequency parametric effects described above, we should satisfy the double-phase-matching conditions. Using the conventional quasi-phase-matching (QPM) technique [9] for FHG via a pure cascade process in $LiTaO_3$, we find that there exists only one wavelength (2.45 μm), for which two parametric processes can be phase-matched simultaneously by the different orders m of the QPM structure with the period $\Lambda_Q = 34$ μm. However, for the so-called phase-reversal QPM structures [10] characterized by two periods, the QPM period Λ_Q and the modulation period Λ_{ph} ($\Lambda_{ph} > \Lambda_Q$), double-phase matching is possible in a broad spectral range, provided the periods are selected to satisfy the conditions $\Lambda_Q = 2\pi(n_1m_2 + n_2m_1)/(\Delta k_1 m_1 - \Delta k_2 m_2)$, $\Lambda_{ph} = 2\pi(n_1m_2 + n_2m_1)/(\Delta k_1 n_1 - \Delta k_2 n_2)$, where (m_1, n_1) and (m_2, n_2) are the grating orders chosen to phase-match the SHG and FHG processes, respectively. If we take $(m_1, n_1) = (-1, -1)$, $(m_2, n_2) = (1, 5)$, and the fundamental wavelength 1.57 μm, then the periods are $\Lambda_Q = 5.027$ μm and $\Lambda_{ph} = 20\Lambda_Q$. With these parameters we found that 92% conversion efficiency into the FH can be achieved in a $L = 1$ cm long crystal at the FF input power of 932 MW/cm^2, as demonstrated in Fig. 2(b) (in dimensionless units). This example illustrates that engineered QPM structures can be very efficient for performing different types of multistep cascading experiments under double-phase-matching conditions. Another possibility recently suggested in Ref. [11] is based on the use of 2D nonlinear $\chi^{(2)}$ photonic crystals.

In conclusion, we have introduced and studied a new model of multistep cascading that describes the fourth-harmonic generation via purely parametric wave mixing. We have analyzed the existence and stability of the stationary solutions of this model for normal modes — plane waves and spatial solitons. We have also discussed the possibility of double-phase matching in engineered QPM structures with phase-reversal sequences.

References

[1] See, e.g., G.I. Stegeman, D.J. Hagan, L. Torner, Opt. Quantum Electron. 28 (1996) 1691.
[2] See, e.g., Yu.S. Kivshar, A.A. Sukhorukov, S.M. Saltiel, Phys. Rev. E 60 (1999) R5056.
[3] K. Koynov, S. Saltiel, Opt. Commun. 152 (1998) 96.
[4] Yu.S. Kivshar, T.J. Alexander, S. Saltiel, Opt. Lett. 24 (1999) 759.
[5] S.A. Akhmanov, A.N. Dubovik, S.M. Saltiel, I.V. Tomov, V.G. Tunkin, Pis'ma Zh. Eksp. Teor. Fiz. 20 (1974) 264, JETP Lett. 20 (1974) 117.
[6] See, e.g., B.A. Hooper, D.J. Gauthier, J.M.J. Madey, Appl. Opt. 33 (1994) 6980.
[7] P.T. Nee, N.C. Wong, Opt. Lett. 23 (1998) 46;
V.G. Dmitriev, S.G. Grechin, in: S. Chesnokov, V. Kandidov, N. Koroteev (Eds.), ICONO '98: Nonlinear Optical Phenomena, Proceedings of SPIE, Vol. 3733, 1998, p. 228.
[8] A.A. Sukhorukov, Phys. Rev. E 61 (2000) 4530.
[9] M.M. Fejer, G.A. Magel, D.H. Jundt, R.L. Byer, IEEE J. Quantum Electron. 28 (1992) 2631.
[10] M.H. Chou, K.R. Parameswaran, M.M. Fejer, I. Brener, Opt. Lett. 24 (1999) 1157.
[11] S. Saltiel, Yu.S. Kivshar, Opt. Lett. 25 (2000) 1204, 1612(E).